Journal of Environmental Chemical Engineering 12 (2024) 112997

Contents lists available at ScienceDirect

Journal of Environmental Chemical Engineering

journal homepage: www.elsevier.com/locate/jece

Navigating the balance between nanofiltration and oxidation to remove organic micropollutants from wastewater treatment plant effluent

Hans David Wendt [a], I. Sena Yaltur [a,b], Dennis M. Reurink [b], Clara Thege [c], Kaspar Groot Kormelinck [c], Joris de Grooth [a,b,*]

[a] Membrane Science and Technology, P.O. Box 217, Enschede 7500 AE, the Netherlands
[b] NX Filtration, Haaksbergerstraat 95, 7554 PA Hengelo, the Netherlands
[c] Van Remmen UV Technology, Hooglandweg 3a, Wijhe 8131 TE, the Netherlands

ARTICLE INFO

Keywords:
Organic Micropollutants
Hollow Fiber Nanofiltration
Advanced Oxidation
Specific Energy Consumption
Molecular Weight Cut-Off

ABSTRACT

The removal of organic micropollutants (OMPs) from wastewater treatment plant effluent is becoming more important due to the adverse effects of these compounds on the environment. To overcome the limitations of currently available technologies, this study proposes a combination of hollow fiber membrane filtration with advanced oxidation to remove OMPs. The possible synergy between these processes was investigated. The nanofiltration membrane ensures the removal of organic matter and thus an improvement of transmittance, after which oxidation with UV/H_2O_2 of the permeate can remove OMPs more effectively and at a significantly lower energy consumption than without a membrane. Six membranes were evaluated with a pure water permeability between 6.7 and 106 $Lm^{-2}\,h^{-1}\,bar^{-1}$ and a $MgSO_4$ retention ranging from 0.93 to 0. The molecular weight cut-off (MWCO) varied from 250 Da to more than 10 kDa. The measured MWCO can depend strongly on the applied flux. The UV-transmittance of NF permeate of treated wastewater was investigated experimentally to be between 97% and 50%. These values were used for an estimation of the specific energy consumption (SEC) for the membrane and the oxidation step, resulting in a combined SEC of 0.17–0.18 $kWhm^{-3}$ for 70 or 80% removal of OMPs, respectively. Remarkably, this lowest SEC was not found for the combination with the most dense membrane, but for a slightly more open membrane. The reported SEC is comparable to the total energy consumption required for ozonation and adsorption, while producing clean water with a double barrier, high transmittance and 70–80% removal of OMPs.

1. Introduction

The quality of important water resources is at risk. One of the concerns relates to the release of organic micropollutants (OMPs) to the aquatic environment. OMPs are small, often very persistent, water soluble, organic molecules, such as pharmaceuticals, personal care products, and endocrine disrupting chemicals. These compounds enter wastewater through excretion from humans and animals, run-off, or direct discharge. Even when wastewater is treated, the removal of OMPs is limited [1–3]. The OMPs therefore remain in the effluent of wastewater treatment plants (WWTPs) and end up in the recipient, typically local surface water. There, OMPs can harm the environment [4,5], or subsequently end up in drinking water sources [3].

To prevent OMPs from entering surface waters, additional treatment is required. Processes based on adsorption, oxidation or filtration are most well-developed [1,6–8]. Adsorption is already used in full-scale plants [9], is typically based on activated carbon, and only transfers OMPs from the water phase to the solid phase; elimination occurs during the regeneration of the material, with a high carbon footprint and high energy costs. Oxidation processes are also already applied at large scales and break the OMPs down chemically. Advanced Oxidation Processes (AOPs), for instance with ozone or hydrogen peroxide, have the potential to fully mineralize the OMPs into mainly H_2O and CO_2, but a notable risk in AOPs is the formation of unwanted metabolites. Finally, while filtration with relatively dense membranes as in reverse osmosis or nanofiltration (NF) is effective at separating OMPs from wastewater effluent into a concentrate, membranes do not eliminate OMPs. The OMPs in the concentrate still need further treatment to ensure a complete removal [10].

The described existing processes all have their drawbacks, but these limitations could be overcome by combining different technologies with

* Corresponding author at: Membrane Science and Technology, P.O. Box 217, Enschede 7500 AE, the Netherlands.
E-mail address: j.degrooth@utwente.nl (J. de Grooth).

https://doi.org/10.1016/j.jece.2024.112997
Received 26 October 2023; Received in revised form 30 April 2024; Accepted 5 May 2024
Available online 16 May 2024

Nomenclature

Glossary

A	Water permeability coeficient [$Lm^{-2}\ h^{-1}\ bar^{-1}$].
B	Solute permeability coefficient [mh^{-1}].
D	UVC dose D in Jm^{-2}.
I_{UV}	UVC intensity in Wm^{-2}.
J_s	Solute flux through the membrane [$mol\ m^{-2}\ h^{-1}$].
J_w	Water flux through the membrane [$Lm^{-2}\ h^{-1}$].
R_{int}	Intrinsic retention [-].
R_{obs}	Observed retention [-].
S	Recovery [-].
$\phi_{v,f}$	Volumetric flow rate of feed stream [$m^3\ h^{-1}$].
$\phi_{v,p}$	Volumetric flow rate of permeate stream [$m^3\ h^{-1}$].
c_b	Concentration in the bulk of the membrane feed stream [mol/m^3].
$c_{f,t=0}$	Concentration of the feed stream at the start of the experiment [mol/m^3].
c_f	Concentration of the feed stream [$mol\ m^{-3}$].
c_m	Concentration at the membrane interface [$mol\ m^{-3}$].
c_p	Concentration of the permeate stream [$mol\ m^{-3}$].
k	Mass transfer coefficient [ms^{-1}].
t_E	Exposure time to UVC dose in s.

each other. Various combinations of oxidation processes and membranes have been reviewed by Titchou et al. [11]. A typical example is the application of ozonation on the concentrate of NF [12–14]. This can improve the degradation of OMPs, but since also bulk organic matter accumulates, which scavenges the oxidant, the reduction in oxidant dosage is limited [15]. Saquib et al. on the other hand treated permeate of an ultrafiltration membrane that was fed with surface water, with ozonation [16]. This yielded no significant improvement in removal efficiency for the single OMP investigated (atrazine). In this case, only one membrane was investigated, which might not have been adapted well for the application at hand. This approach can lead to combinations that are not optimized and do not utilize the full synergy between two technologies, which can lead to suboptimal energy consumption and OMP removal.

The goal of this work is to investigate the synergetic potential of membrane filtration and advanced oxidation, in which both technologies are adapted to each other. After typical biological treatment in a WWTP, the first step is the treatment of effluent with a hollow fiber NF membrane. This membrane should retain the majority of bulk organic matter that is still present in the treated wastewater, which absorbs UVC light. This aim is due to the sensitivity of AOPs to the composition of the water [15,17–20]. The main parameter that affects the efficiency is the interference from bulk organic compounds in the water matrix due to adsorption of the UVC light or the ozone. The obtained permeate should have a significantly increased UVC-transmittance, to ensure a lower energy consumption in the oxidation step.

Instead of only combining two technologies, multiple membranes are investigated to find the most optimal combination with the oxidation process, with the goal of finding the lowest energy consumption. The ideal membrane for this process still has a high permeability, but should also retain compounds that decrease the UVC-transmittance. Hollow fiber membranes are specifically chosen to be investigated since significant pre-treatment of the effluent is not required before filtration [21]. This is in contrast to spiral-wound membranes, which require pre-treatment with e.g. ultrafiltration membranes [22]. Only the permeate of the membrane will be considered; in practice, treatment of the concentrate will be necessary as well, and could potentially be done by recycling it back to the WWTP similar to Kappel et al. [23].

As already indicated, the main types of AOPs use UVC light and hydrogen peroxide or ozone [17]. Oxidation with ozone carries a risk for the formation of carcinogenic by-products, such as bromate and N-nitrosamines [24–26]. The UV/H_2O_2 process also creates by-products in the form of metabolites, that may be toxic [27]. However, several tests show no effect, or a decreasing effect, on toxicity [28–30]. Furthermore, the formation of metabolites can be reduced by adapting the process conditions, e.g. UVC dosage [31]. Because of the smaller negative side effects, we propose to use UV/H_2O_2 over ozonation as oxidation step.

With the positive effect of NF membranes on the transmittance of the water, the aim is to find a synergy between UV/H_2O_2 and NF membranes, potentially resulting in lower energy consumption for the treatment as a whole. The NF membrane should increase the transmittance of the water, leading to lower energy consumption for the oxidation step compared to not using a NF pre-treatment step. The energy consumption of the NF step itself might then be lower than for dense NF membranes, typically envisaged to be used to remove OMPs in one step. This work specifically aims to find a point where both technologies are well adapted to each other, leading to a lower energy consumption for both technologies combined compared to a single technology. Furthermore, with the treatment of the effluent by a double barrier process with NF and oxidation, the obtained product water is expected to have a high quality, leading to possibilities for reuse for irrigation purposes, process water, or potentially even drinking water quality.

The goal of this work is to investigate the synergistic relation between membrane apparent pore size and the subsequent AOP to come to a total solution with a lower specific energy consumption. Typical membrane characterization parameters are reported first, based on synthetic laboratory solutions, to obtain data on the membrane performance. Six different membranes are characterized for permeability, $MgSO_4$ retention, and molecular weight cut-off (MWCO). All these experiments are performed at different pressures and corresponding fluxes, to be able to investigate the effect of flux on the characterization. After that, the performance of the membranes with effluent from a WWTP as feed is described. The transmittance of the permeate is determined at different recoveries or concentration factors, to determine suitable operation parameters. The obtained recovery and transmittance data are used in a specific energy consumption (SEC) analysis, where the energy consumption of both the membrane and the oxidation step are determined to obtain a removal of a mixture of OMPs of 70 or 80%. Based on the total SEC, the most promising membrane for this process is identified, and a comparison is made to other available technologies.

2. Materials and methods

2.1. Chemicals and materials

Six different hollow fiber membranes were experimentally investigated. All membranes were kindly provided by NX Filtration B.V. (Enschede, The Netherlands). The most open (UF010) and most dense (dNF80) membrane are commercially available [32]. Four different membranes with a permeability between these two extremes have been prepared by coating polyelectrolyte multilayers (PEM) on the UF010 membrane. The different membranes were prepared by coating an increasing amount of polyelectrolyte multilayers on the fibers, following the procedure from [33]. In all cases, the coating was terminated with a polyanion step in 0.05 M NaCl, rendering all membranes negatively charged. These four membranes will be referred to as M-1 (most open after UF010) up to M-4 (most dense after dNF80).

$MgSO_4 \cdot 7\ H_2O$ was obtained from Vivochem B.V. Diethylene glycol was obtained from Sigma-Aldrich, whereas all other PEGs were obtained from Merck. Effluent was obtained from the wastewater treatment plant of Glanerbrug, The Netherlands. Characteristics of the effluent are reported in Table S4.

2.2. Membrane characterisation

The membranes were always operated in inside-out crossflow configuration. The permeability, $MgSO_4$ retention (at 5 mM), and MWCO of the membranes were determined with a crossflow set-up, using 10–12 modules of 10–15 cm in length with 3 fibers per module (see Figure S1). The permeate was obtained for analysis, while the concentrate was returned to the feed vessel of 5 L. The setup includes pressure sensors, temperature sensors and flow sensors to measure the required process parameters. A cross-flow velocity of 0.5 ms^{-1} was used throughout the experiments. The pure water permeability and $MgSO_4$ retention experiments were performed at room temperature. Permeability values were normalized to 20 °C by accounting for the change in viscosity. Pure water permeability was measured using ultrapure water (conductivity of 5 μS cm^{-1}) at transmembrane pressures ranging from 0.5 to 5 bar. The observed retention (R_{obs}) was calculated with Equation (1), where concentration was determined based on conductivity.

$$R_{obs} = 1 - \frac{c_p}{c_f} \tag{1}$$

To determine the MWCO, two different mixtures have been used with 1 gL^{-1} of different molecular weights of polyethylene glycol (PEG). The two mixtures were used to be able to distinguish the different peaks of different PEG molecular weights in a GPC assay. Mixture A includes diethylene glycol and PEG with a molecular weight of 400 Da, 1 kDa, 4 kDa, 10 kDa and 35 kDa. Mixture B includes PEG with a molecular weight of 200 Da, 600 Da, 2 kDa, 6 kDa and 20 kDa. The MWCO experiments are performed at room temperature. The membranes were operated at such transmembrane pressures that the flux of all the membranes was in a range of 10–60 $Lm^{-2}h^{-1}$.

Samples of 6 of the original 12 modules per membrane type were selected randomly for gel permeation chromatography (GPC) analysis. Signals were corrected for the baseline of the eluent (25 mg/L of NaN_3), which interfered around a molecular weight of 10 kDa. The analysis is done with a size exclusion column (two Polymer Standards Service Suprema 8 × 300 mm columns in series: 1000 Å, 10 μm and 30 Å, 10 μm). The eluent is 50 mgL^{-1} of NaN_3 in water at a flow rate of 1 mL min^{-1}. The observed retention of the compounds is again determined with Equation (1), with a linear relationship between the refractive index signal and concentration.

For the interpretation of the results, it is important to distinguish between the observed and the intrinsic retention. The observed retention is not always similar to the intrinsic retention as defined by Equation (2), because of concentration polarization taking place in the boundary layer close to the membrane. To explain this, the same manner is used as by Platt et al. [34]:

$$R_{int} = 1 - \frac{c_p}{c_m} \tag{2}$$

Using the film model, the concentrations in the boundary layer can be calculated with Equation (3):

$$\frac{c_m - c_p}{c_b - c_p} = \exp\left(\frac{J_w}{k}\right) \tag{3}$$

By substituting Equation (2) into Equation (3), one obtains a quantification of the concentration polarisation (CP) modulus as in Equation (4):

$$\frac{c_m}{c_b} = \frac{\exp\left(\frac{J_w}{k}\right)}{R_{int} + \left[1 - R_{int}\exp\left(\frac{J_w}{k}\right)\right]} \tag{4}$$

If the intrinsic retention approaches 1, Equation (4) reduces to Equation (5).

$$\frac{c_m}{c_b} = \exp\left(\frac{J_w}{k}\right) \tag{5}$$

Using the intrinsic retention and the permeability, one can define the water permeability parameter coefficient A and the solute permeability coefficient B for dense membranes [35], as shown in Equations (6)-(7):

$$J_w = A(\Delta P - \Delta\pi) \tag{6}$$

$$J_s = B(c_m - c_p) \tag{7}$$

The MWCO is defined in this work as the point where the observed retention equals 0.9.

2.3. Membrane tests with effluent for UVC-transmittance and LC-OCD

The experiments with effluent were performed with larger-scale modules of the same six different membrane types, with around 120 fibers per module and a module length of approximately 30 cm (see Figure S1). This yields, depending on the exact length between potting, a membrane area of 0.05–0.06 m^2 per module. The experiments are performed with a Mexplorer setup, obtained from NX Filtration B.V. (Enschede, the Netherlands), containing a feed pump with frequency controller, a flow meter to check crossflow velocity and a concentrate needle valve to control the transmembrane pressure. The flux varied from 30 $Lm^{-2}h^{-1}$ LMH for the dNF80 membrane to 60 $Lm^{-2}h^{-1}$ for UF010. A consistent crossflow velocity of 0.5 m/s was used. The system was recirculated with effluent for 1 h to stabilize. After that, the permeate was continuously discharged, leading to an increase in recovery over time. Recovery in the batch experiments is calculated as $V_p/V_{f,0}$. Conductivity and UVC transmittance at 254 nm (UVT_{254}) of the feed and permeate were determined at recoveries of 0, 0.3, 0.5, 0.8, and 0.9. Conductivity was determined with a Hanna Instruments HI99300 portable conductivity meter with probe HI763063, and UVT_{254} with a RealTech P200 portable transmittance analyzer. Samples for Liquid Chromatography - Organic Carbon Detection (LC-OCD) were taken at the start of the experiment and at a recovery of 0.8. The temperature ranged from 6 to 28 °C during the experiments, since the solutions were taken from the fridge and heated by the pump during experiments. Permeability values were normalized to 20 °C by accounting for the change in viscosity. After each experiment, the set-up and membrane module were cleaned with a 200 ppm NaOCl solution at pH 11.

LC-OCD experiments were performed to determine which fractions of organic matter were retained by the different membranes used. After running the sample through a size exclusion column, the OCD can detect components that are UVC-inactive and with that, quantify the different TOC-fractions as biopolymers, humic substances, building blocks, low molecular-weight acids, low molecular-weight neutrals, and hydrophobic organic carbon [36,37]. The samples were sent to 'Het Waterlaboratorium' in Haarlem, the Netherlands for analysis. The passage of different fractions was calculated with Equation (8).

$$\text{Passage} = \frac{c_p}{c_{f,t=0}} \tag{8}$$

3. Calculations

The experiments in this work are combined with calculations for a Specific Energy Consumption (SEC) analysis for both the membrane and oxidation step. These calculations are explained below.

3.1. Membrane

A realistic base case scenario is assumed with all membrane modules in parallel in one stage, at a crossflow velocity of 0.3 m/s. The crossflow velocity is maintained by recirculating part of the concentrate to the feed of the membranes in the so-called feed & bleed mode. The

experiments were performed at a crossflow velocity of 0.5 ms^{-1}, but 0.3 ms^{-1} is chosen here because this is a more realistic value for full-scale operation. The permeability of the different membranes is assumed to be independent of recovery. In the calculations, the lowest permeability value during the effluent experiments is taken. A suitable operating flux is determined based on the permeability of the membrane assuming an operating temperature of 20 ˚C, leading to a trans-membrane pressure of the membranes of approximately 2 bar for all cases. The permeability and flux numbers used for the calculations can be found in Table S1.

The pressure drop is calculated with the Darcy-Weisbach equation in a module of 1.5 m, with an inner fiber diameter of 0.7 mm and the density of pure water. To make sure that the average transmembrane pressure equals the feed pressure, half of the pressure drop is added to determine the power of the feed pump. The permeate flow rate is the same for all membrane types, whereas the feed flow rate in the continuous process depends on the recovery (S), as depicted in Equation (9). To make sure the desired crossflow velocity is achieved, the power of a recirculation pump is determined by calculating the recirculation flow and assuming the pressure drop needs to be overcome. Pump and motor efficiency are taken into account and estimated to be both 90%, based on elementary design principles for centrifugal pumps [38], leading to a total efficiency of 81%. The corresponding flow sheet and equations can be found in S1.

$$\phi_{v,f} = \frac{\phi_{v,p}}{S} \tag{9}$$

3.2. Oxidation

The most important factors to determine the energy consumption of the UV/H_2O_2 system are the UVC-transmittance at 254 nm and the targeted removal efficiency. First, the relevance of UVC-transmittance as main model parameter are discussed. After that, the UVC-transmittance is linked with a UVC dose for the required OMP removal.

3.2.1. Relevance of UVC-transmittance

The relevance of UVC-transmittance in the model is twofold: UVC-transmittance directly affects the application of the UVC dose, and it acts as an indicator of hydroxyl radical scavenging behavior [39,40]. The UVC dose D in Jm^{-2} is built up by the UVC intensity I_{UV} in Wm^{-2} and the exposure time t_E in s, as shown in Equation (10) [41].

$$D = I_{UV} \cdot t_E \tag{10}$$

The UVC intensity is affected by the UVC output of the UVC lamp(s), the thickness of the water layer, and the composition of the water measured as UVC-transmittance. The exposure time is affected by the flow management design of the UVC reactor and the flow rate [41,42]. Regardless of the UVC reactor, per finalized UVC reactor design, only the UVC-transmittance (part of I_{UV} in Equation (10)) is unknown as the others are fixed constants.

The UVC-transmittance is determined by the composition of the water, meaning all organic and inorganic compounds and ions in the water matrix that absorb UVC light. Higher absorbance reduces the UVC-transmittance which overall lowers the final UVC light intensity, leading to a required increase of the exposure time for an equal UVC dose, resulting in a lower flow rate and higher energy consumption.

The largest contributor to a decrease in UVC-transmittance is an increase in the dissolved organic carbon (DOC) or total organic carbon (TOC) content of the water [19,43]. The relationship between DOC or TOC and UVC-transmittance is well known [19]. UVC-transmittance can be used to identify composition as well, as it has a strong correlation with the aromaticity content [44]. The real relationship between the UVC-transmittance and the DOC or TOC is unique to each water [19] but typically has an absorbance of 80–350 mol L^{-1} cm^{-1} [43].

Besides organic compounds, inorganic compounds present in the water also have an effect on the UVC-transmittance. Iron can be present, especially when iron is dosed in an upstream process in the WWTP. It is known to contribute to UVC absorbance, where ferric and ferrous iron have an absorbance of 3069 and 466 mol L^{-1} cm^{-1}, respectively [43]. Iron containing compounds are also known to interfere with UVC based DOC and/or TOC measurements [19,45]. Other inorganic compounds common in wastewater such as nitrate, hypochlorite, and zinc ions have a smaller absorbance in comparison, 1.7–29.5 mol L^{-1} cm^{-1} [43].

Well-known hydroxyl radical scavengers are hydrogen peroxide or hydrogen peroxide ion, carbonate or bicarbonate, phosphate, nitrite ions, bromide ions, and DOC [46]. Other compounds that have a negative impact on the UV/H_2O_2 process and can be inferred as having a scavenging effect are cations, such as sodium, calcium, magnesium, and copper [39]. Among these scavengers, several show UVC-light absorbance of 18–230 mol L^{-1} cm^{-1} [40,43,47–49]. The actual significance of the effect on the UVC-transmittance is a question of abundance, as seen with DOC or TOC [43]. The hydroxyl scavengers can thus be assumed to be partially compensated for by the UVC-transmittance, which adds to the relevance of the UVC-transmittance as main parameter in the model.

pH can also affect the hydroxyl radical formation and the effectiveness of the formed radicals [39] or affect the absorbance [50,51]. However, the UV/H_2O_2 process has shown to be successful in the pH range of 5–9 with a preference for pH< 7 [39,52,53]. Typically, the pH of wastewater effluent is regulated in a relatively small window, between 6.5 and 8.5 [43]. The pH can thus be assumed to either be irrelevant or to be partially compensated for by the UVC-transmittance.

It should be noted that not all compounds and ions that absorb UVC light lead to a reduction in treatment effectiveness and increase in energy consumption. For instance, due to a photocatalytic effect of target OMPs or interactions between the UV/H_2O_2 process and the presence of Fe^{2+} or Fe^{3+} iron, more hydroxyl ions are generated [46,54]. Carbonate and phosphate have also shown to aid in the degradation by the generation of secondary radicals [55]. On the other hand, more difficult to oxidize OMPs can increase the energy consumption also at higher UVC-transmittance.

Overall, the UVC-transmittance captures many contaminants and is a good measure to predict energy consumption in UV/H_2O_2 oxidation for indicative purposes. It is useful to compare the different membrane permeates in this study, and can give a good estimate for other water matrices, if their characteristics are similar to the matrices that are used for the model. The values for UVC-transmittance of the permeate, and thus of the feed of the UV/H_2O_2 system, are taken from the membrane experiments with effluent of this work.

3.2.2. UVC dose determination

To accurately analyze the energy consumption of the oxidation part at the targeted 70 and 80% average OMP removal in different transmittance scenarios, the UVC dose required for this removal efficiency needs to be determined. That UVC dose together with the transmittance dictates the capacity of UVC reactor with known energy consumption. Both 70 and 80% removal efficiency are considered in this work, since the current goals of several countries for final removal are in this range [56,57]. It is assumed that the membranes do not remove any OMPs, although it is known that e.g. the dNF80 membrane can partly retain OMPs [58]. However, this assumption makes the calculations a worst-case scenario in which the oxidation has to remove all OMPs, combined with the fact that the effective removal of the membrane might be relatively low if the concentrate is recirculated to the WWTP due to accumulation there.

Four studies with a total of 64 OMPs, focused on pharmaceuticals and other medicinal residues, were reviewed at UVC transmittance levels ranging from 50% to 95%. These studies were selected because all of them are performed on real water matrices, and all except [28] with similar Van Remmen Advanox™ UVC reactors. In the interest of reducing the effect of potential outliers, overlapping OMPs were

reviewed, representative of the larger population of OMPs. Among the 64 OMPs, 18 overlapped in two or more studies [28,29,31,59]. UVC and hydrogen peroxide doses were compared and interpolated for all of these compounds. The approach is shown below for an excerpt of five OMPs, with in Table 1 the removal for different values of transmittance, H_2O_2 dose and UVC dose based on literature. The UVC reactor geometry used in [28] was used to determine the approximate average UVC dose in that work, as the reported UVC dose only accounted for the minimum UVC dose. For the other references, the average UVC dose was directly taken.

Based on the data of Table 1 and the fits shown in Figure S4, the average UVC and H_2O_2 doses required for 70% removal for the 5 excerpt compounds are $<$ 12000 Jm^{-2} at 50% UVC transmittance with 30 mgL^{-1} H_2O_2 [28]; 5566 Jm^{-2} at 60% UVC transmittance with 22 mgL^{-1} H_2O_2 [29]; 5000 Jm^{-2} at 70 % UVC transmittance with 25 mgL^{-1} H_2O_2 [59]; and 690 Jm^{-2} at 95% UVC transmittance with 10 mgL^{-1} H_2O_2 [31]. For 80% removal, this changes slightly to $>$ 12000 Jm^{-2} at 50% UVC transmittance with 30 mgL^{-1} H_2O_2 [28]; 7899 Jm^{-2} at 60% UVC transmittance with 22 mgL^{-1} H_2O_2 [29]; 5000 Jm^{-2} at 70% UVC transmittance with 33 mgL^{-1} H_2O_2 [59]; and 1641 Jm^{-2} at 95% UVC transmittance with 10 mgL^{-1} H_2O_2 [31].

In the review of all 64 compounds, the same comparison was made for different UVC and H_2O_2 doses. A minimal difference was found in removal efficiency compared to UVC and H_2O_2 dose setting between the analysis of all 64 compounds, or the 18 overlapping compounds, with a maximum of 5% deviation. As this study uses no specific target compounds, further calculations are simplified by using the results from the analysis of all 64 compounds. These values, together with respective standard deviations based on spread in removal efficiency, can be found in Table 2 and are fitted in Figure S5. In all cases, the UVC dose and H_2O_2 dose deviation were within a deviation of less than 20%. Furthermore, the values are very similar to the excerpt results with only five compounds.

3.2.3. UVC reactor capacity

In determining the capacity of a UVC reactor, it is assumed that a Van Remmen Advanox™ Flow UVC reactor, using low-pressure UVC lamps, is used. Characteristics of this reactor are given in section S1. This reactor is designed based on previous research [60] specifically for AOP with UV/H_2O_2 with a focus on dose distribution and flow management. Computational Fluid Dynamics (CFD) calculations supported by kinetic modeling [61] were used to determine the capacity of the Advanox Flow UVC reactor at several transmittance values. A mathematical light field analysis combined with the CFD data was used to determine the reactor capacity and UVC dose at any given transmittance.

Due to the inversely proportional relationship between exposure time and UVC dose, only one UVC dose and capacity combination per transmittance point is required for conversions to different UVC doses or flows, within the constraints of the minimum and maximum design UVC dose of the system. For example, if at a UVC-transmittance of 60%, the light field and CFD calculations gave a flow of 150 m^{-3} h^{-1} for a UVC dose of 5000 Jm^{-2}. Doubling the flow through the reactor reduces the UVC dose by a factor of two and vice versa: at the same transmittance, 300 m^{-3} h^{-1} gives 2500 Jm^{-2} and 75 m^{-3} h^{-1} gives 10000 Jm^{-2}, respectively. The same relationship between UVC dose and flow is true regardless of transmittance. The CFD calculations are run several times per transmittance point with variations in flow to account for flow management deviations. Reactors designed through this method, including Advanox Flow, have been piloted on-site [31] and capacities confirmed to match the modeling.

Figure S6 shows the capacity of the UVC reactor at the UVC doses required for 70 and 80% average OMP removal. For this configuration of doses, the hydraulic maximum per reactor (800 m^{-3} h^{-1}) is met around 90% transmittance. The SEC assumes a flow perfect for the UVC dose, meaning no arbitrary flow was set for the calculation. In a real-life scenario, the number of reactors would need to be rounded up. The SEC of the oxidation step can be calculated by dividing the power supplied to a reactor with the reactor capacity and is shown in Fig. 1.

4. Experimental results & discussion

In this section, the characterization of the different membranes is described first, showing their different levels of water permeability and solute retention capabilities. Next, the results of using these membranes to treat effluent of a wastewater treatment plant are described.

4.1. Pure water permeability

The aim of this work is to test membranes with different levels of permeability and adapt them to the oxidation process. This difference is well reflected in the pure water permeability, which is depicted in Table 3. The results of the pure water flux versus, which form the basis of Table 3, are presented in Figure S7. The results are in line with expectations and show that a relatively broad range of permeability is obtained, with all membranes having substantially different permeability.

4.2. $MgSO_4$ retention

The retention of the different membranes for 5 mM $MgSO_4$ is shown as a function of flux in Fig. 2, and as a function of pressure in Figure S8. The order of retention follows the order that could be expected based on the data for permeability, with hardly any retention for the membranes with high permeability and a high retention of up to 0.93 for the densest membrane used (dNF80) at a pressure of 4 bar and a flux of 31 $Lm^{-2}h^{-1}$. The biggest difference in retention is obtained between membranes M-3 and M-4.

The data also shows that the retention of the two most dense membranes (dNF80 and M-4) increases with flux, as can be expected for dense membranes based on the solution-diffusion model described in Equations (6)-(7). The equations imply that a higher transmembrane pressure (TMP) leads to a higher water flux, but at low CP moduli (Equation (4)) the solute flux is not affected by the higher flux. This results in higher retention. The four other, more open membranes do not show a clear increase or decrease in retention for the range of flux measured.

Table 1
Excerpt of removal efficiency data for five compounds at different UVC transmittance levels at constant H_2O_2 concentrations and different UVC doses.

UVT_{254} [%]	50 [28]	60 [29]		70 [59]		95 [31]		
H_2O_2 dose [mg/L]	30	22		20	40	10		
UVC dose [Jm^{-2}]	12000	3000	10000	5000		7300	4870	3650
Carbamazepine	75%	54%	91%	62%	88%	95%	90%	88%
Hydrochlorothiazide	86%	54%	92%	61%	85%			
Metoprolol	75%	56%	67%	66%	90%	98%	90%	85%
Naproxen	100%	77%	100%			98%	98%	95%
Ibuprofen	77%	52%	95%	66%	94%			
Average	78%	59%	89%	64%	89%	97%	93%	89%

Table 2
Overview of results for UVC dose and H_2O_2 dose for different scenarios based on investigating all 70 OMPs. The standard deviation in the calculated values indicates a compound-specific spread in removal efficiency.

UVT_{254} [%]	Case	UVC dose [Jm^{-2}]		H_2O_2 dose [mg/L]		References
		70% removal	80% removal	70% removal	80% removal	
50	Treated wastewater	10054 ± 2011	11363 ± 2273	29.0 ± 5.8	36.6 ± 7.3	[28]
60	Treated wastewater, post sand filter	7274 ± 1018	8858 ± 1240	21.2 ± 3.0	27.8 ± 3.9	[29]
70	Treated wastewater, optimized biology	5533 ± 332	6905 ± 414	16.3 ± 1.0	21.1 ± 1.3	[59]
95	Raw drinking water, pre final polishing	3218 ± 451	3704 ± 519	9.6 ± 1.3	10.6 ± 1.5	[31]

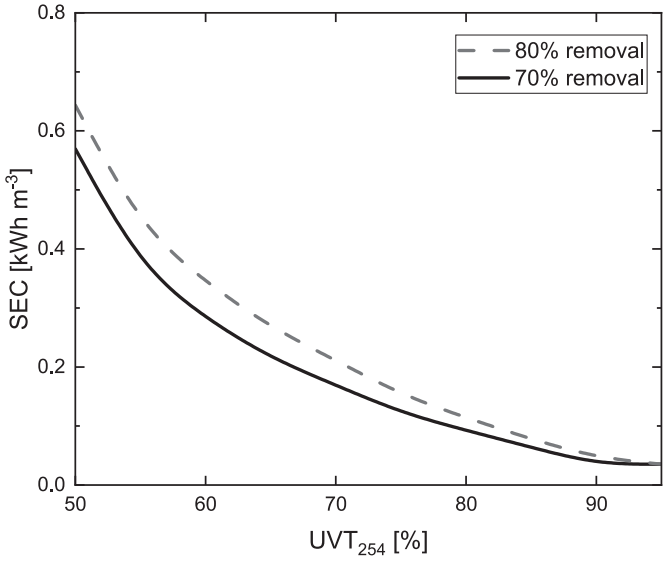

Fig. 1. Specific energy consumption of the oxidation step based on transmittance.

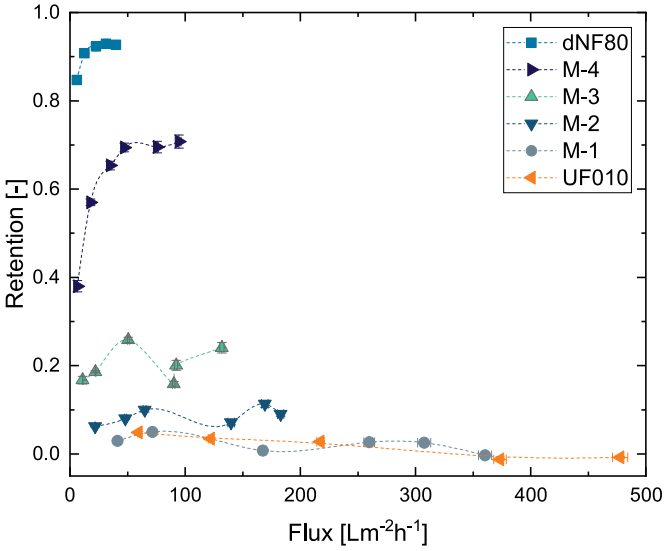

Fig. 2. Retention versus water flux plot for $MgSO_4$. Lines are for visualization purposes only. Error bars indicate the standard error of 12 modules.

Table 3
Pure water permeability (PWP) of the different membranes with standard deviation of 12 modules at 5 different pressures.

Membrane	PWP [$Lm^{-2}\ h^{-1}\ bar^{-1}$]
UF010	106 ± 13
M-1	67.0 ± 3.4
M-2	35.1 ± 3.9
M-3	25.3 ± 3.5
M-4	15.5 ± 1.4
dNF80	6.7 ± 1.7

4.3. Molecular weight cut-off

Typically, the MWCO is reported as one single number for a certain membrane and defined for a model compound that has a retention of 0.9. However, as explained earlier, the retention of a solute depends on the applied process conditions, and as such the apparent MWCO will depend on process conditions or used concentrations of solutes [62–64]. This section provides an investigation of the dependence of the MWCO on the flux. This more in-depth analysis of the separation characteristics or MWCO at different fluxes is relevant for this work since membranes with substantially different permeability are used. These will be operated at different fluxes in applications, which can lead to different results.

To be able to separate the individual PEG peaks in the GPC analysis, two different mixtures have been prepared. The results with the final determination of the MWCO for one of the mixtures are presented in Fig. 3. The other mixture can be found in Figure S9. Due to variations in flux between mixtures A and B at the same applied pressure, it is not possible to combine measurement points at the same pressure into a single molecular weight per flux value. The same trends can be deduced from both mixtures and will be explained below, based on mixture B.

In Fig. 3, it can be seen that the observed MWCO is indeed dependent on the process conditions. For the two most open and two most dense membranes, the MWCO strongly depends on flux. The two most open membranes show a strong increase in MWCO with an increase in flux. This means that the retention for the PEGs that are relevant for the MWCO decreases with increasing flux. This can be attributed to the concentration polarization in the boundary layer. Since the definition of MWCO used is at a relatively high retention of 0.9, the simplified expression as presented in Equation (5) can be used for further explanation. If the flux is increased substantially, this equation shows that the CP modulus increases as well for a similar mass transfer coefficient.

The more open membranes have a relatively high MWCO. At this higher molecular weight range, the CP modulus is higher, due to the lower diffusion coefficient for a higher molecular weight solute. As the calculations in Table S2 show, the CP modulus is 1.9 at the lowest flux reported for UF010 (18 $Lm^{-2}h^{-1}$) with a diffusion coefficient estimated at the MWCO (7.8 kDa). This increases to a CP modulus of 2.5 for the highest flux reported for UF010 (41 $Lm^{-2}h^{-1}$ and MWCO of 12.6 kDa). These calculations do not take into account the formation of a fouling layer of the PEGs at the membrane surface, which can lead to a lower diffusion coefficient of the PEG close to the membrane, increasing the CP modulus further. The fouling layer is evidenced by a clear decrease in permeability when the measurements are performed with PEGs instead of $MgSO_4$, with lower fluxes at equal TMP (data not shown).

The effects described above lead to a much lower observed retention, and thus to a higher observed MWCO. Apart from the theoretical explanation, it is also again illustrated that the thin PEM on M-1 does not increase the capability to retain compounds compared to the support

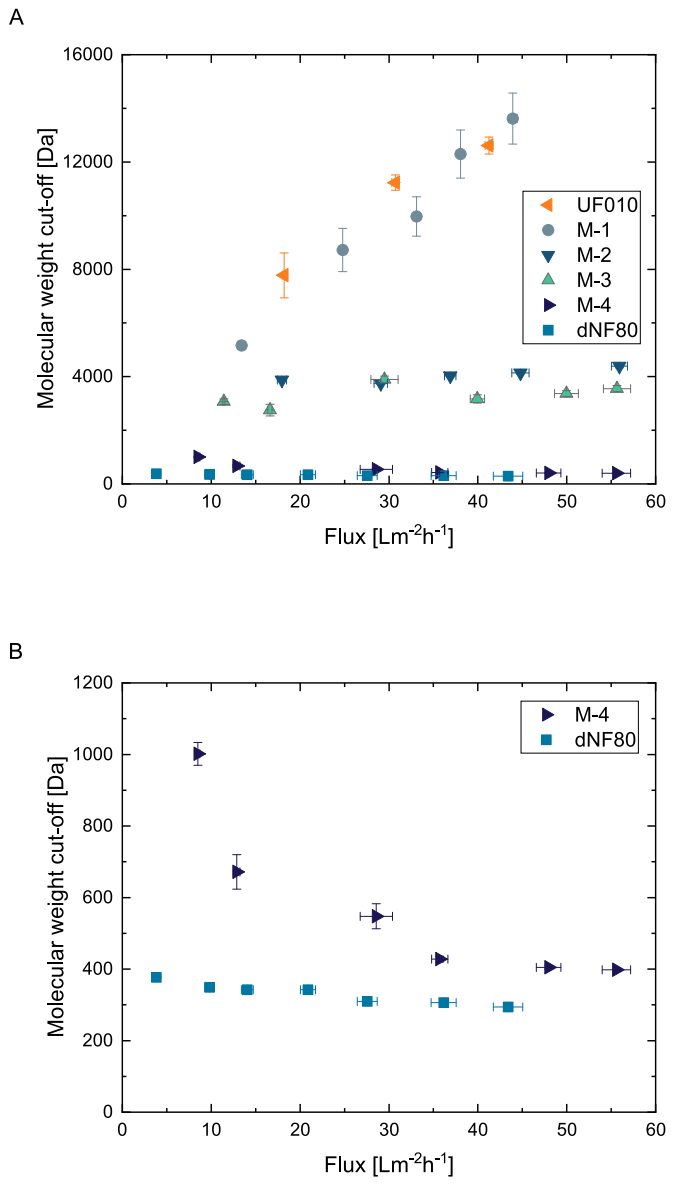

Fig. 3. Flux dependence of molecular weight cut-off for the six membranes used in this study for mixture 2 (A), focused on the two most dense membranes (B). Error bars indicate the standard error of typically six modules.

material UF010, just as with the $MgSO_4$ retention. Given the lower permeability of M-1 compared to UF010, UF010 would be preferred for virtually any application.

The MWCO of membranes M-2 and M-3 is reasonably stable over the range of flux measured, whereas the two most dense membranes show a decreasing MWCO with an increase in flux. In other words, the retention of the membranes increases with flux. This corresponds with the solution-diffusion model, as explained already for the retention of $MgSO_4$. The impact of concentration polarization, as discussed for the more open membranes, is not as pronounced for the dense membranes, due to the smaller molecular weight of the relevant PEG compounds for the MWCO and their correspondingly higher diffusion coefficients. Correspondingly, CP moduli for the dNF80 membrane were calculated to range from 1.1 to 1.9 in the relevant range for the MWCO, as shown in Table S2. The dNF80 membrane shows a decrease in MWCO with an increase in flux to a smaller extent, which might be attributed to the fact that the largest effect is visible at even lower fluxes than measured. Furthermore, the MWCO of the dNF80 membrane is in all cases below 400 Da. Based on literature with PEM membranes with a similar MWCO and their effective pore size of 0.3–0.5 nm, the pore size of the dNF80 membrane is expected to be well below 1 nm [65]. The fact that the M-2 and M-3 membrane show a stable MWCO might be caused by a balance between the beneficial effect of a higher flux for retention, and the increase in CP modulus.

The above-mentioned observations have implications for operation in full-scale applications for the desired fluxes. Within reasonable limits, an open membrane is preferably operated at rather high fluxes, 50 $Lm^{-2}h^{-1}$ or higher, but this data shows that the MWCO can vary more than a factor two between a flux of 50 and a flux of 15 $Lm^{-2}h^{-1}$, thus retaining fewer compounds at higher flux. For the dense membranes, the implications are less impactful, since such membranes typically are operated at fluxes of at least 20 $Lm^{-2}h^{-1}$, at which the MWCO is already close to a stable value at the measured conditions.

The MWCO is an extract of the results for the retention of PEG-molecules with a range of molecular weights. An example of more detailed results can be seen in Fig. 4 for the UF010 membrane. It can be seen that for PEG with a relatively low molecular weight, e.g. 400 Da and 1 kDa in this case, the retention slightly increases with flux. However, the bigger molecules, such as the PEG with molecular weights 6 and 35 kDa, follow a different pattern and show a decrease in retention as flux increases. The intermediate PEG displayed here, with a molecular weight of 2 kDa, seems to show an increase at first, but then a decrease in retention with flux, showing both of the behaviors described before. These results support the previous discussion on the effect of the molecular weight and the corresponding diffusion coefficient in the boundary layer, leading to significant (larger molecules at higher flux) or insignificant (smaller molecules at lower flux) concentration polarization.

4.4. *Membrane performance with effluent*

The key question in this research is the ability of the membranes to retain components that have a negative effect on the permeate transmittance, to decrease the specific energy consumption of the subsequent oxidation step. Based on the insights from the six different membranes of this study, the economic analysis can be performed in the next section. The membranes that were used for effluent tests were from another batch than the results described so far and contained more and longer fibers. $MgSO_4$ retention and permeability showed comparable results to the results shown before, as can be seen in Table S3 and Figure S10.

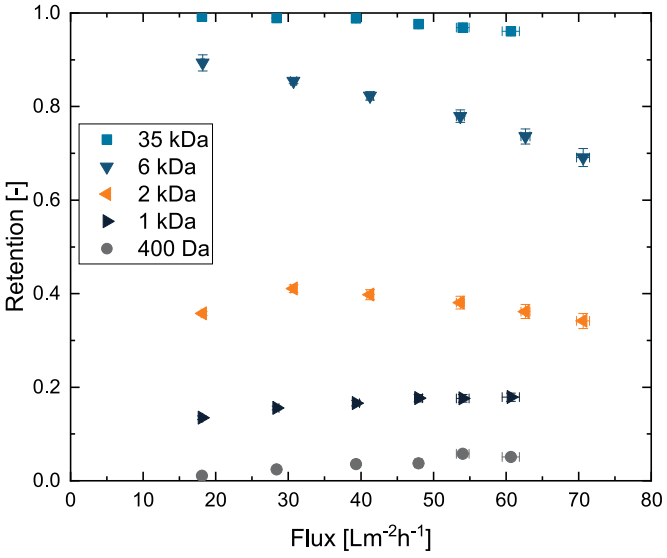

Fig. 4. Retention versus flux analysis with different sizes of solutes for the UF010 membrane. Error bars indicate the standard error of typically six modules.

The transmittance of both the feed and the permeate is shown in Fig. 5. It can be seen that the permeate transmittance is in accordance with the results of permeability, $MgSO_4$ retention, and MWCO. The dNF80 membrane ensures the highest permeate transmittance, and UF010 the lowest. Even more, the initial feed for UF010 possessed the highest transmittance, but still the transmittance of the permeate at the start of the experiment is the lowest value measured. It also appears that the transmittance of the M-1 is not substantially higher than for the UF010 membrane. Combined with the lower permeability of M-1 compared to UF010 and the very similar MWCO, this means that the M-1 membrane is not very attractive to use compared to the UF010 membrane in the envisaged process. This might be attributed to defects in the selective layer of M-1 that can be present, due to the lowest number of applied PEMs in this study. Finally, Fig. 5 shows that the permeate transmittance decreases as the recovery increases, which is expected due to the decreasing feed transmittance.

Relating back to the results for the MWCO, it is interesting to see that the permeate transmittance for membrane M-3 is clearly higher than that for M-2, even though the feed of M-3 has the lowest transmittance of all experiments, and even though the flux for these two membranes was very similar. In the MWCO results, there was hardly any difference visible between M-2 and M-3. This shows that only measuring the MWCO gives limited insight into the performance of different membranes for real applications, or at least in this case for the transmittance of the permeate. However, based on the current results, it appears that promising membranes to significantly improve the permeate transmittance might be found in a range below 2000 Da, and that a much higher MWCO (4000 Da or higher) seems not to be able to do this. The range between 2000 Da and 4000 Da is more dependent on flux and the limitations of the MWCO, both effects described before. In all these comparisons, the flux is a relevant parameter. The flux for the experiments was close to 60 $Lm^{-2}h^{-1}$ for UF010 and M-1, close to 40 $Lm^{-2}h^{-1}$ for M-2, M-3 and M-4, and close to 30 $Lm^{-2}h^{-1}$ for dNF80. This means that UF010 and M-1 were operated at a flux with a relatively low MWCO and therefore suboptimal separation properties, whereas the other membranes were measured at their stable or optimal range of flux, according to the MWCO data.

The results of the LC-OCD analysis confirm the findings on the MWCO and the transmittance. The passage of Total Organic Carbon (TOC) is shown in Fig. 6. There is a clear decrease in the passage of TOC with denser membranes, with the most significant decrease between M-3 and M-4. Furthermore, there is hardly a difference in TOC passage between the UF010 and M-1 membranes. It also is clear that the TOC passage is higher at a reasonable recovery (80% in this case) compared to the TOC passage at the start of the experiment. This is due to the continuous increase of the feed concentration during these tests. This shows that an overestimation of membrane performance can happen at low recovery in lab settings. All of these findings correspond with the results for the UVC-transmittance.

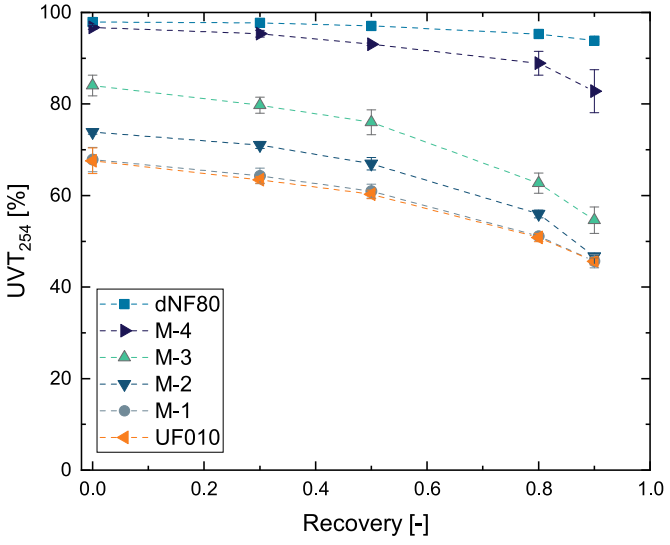

Fig. 5. UVC transmittance of the permeate for all membranes with effluent with a transmittance between 30% and 41% initially. Lines are for visualization purposes only. Error bars indicate the standard error of two runs.

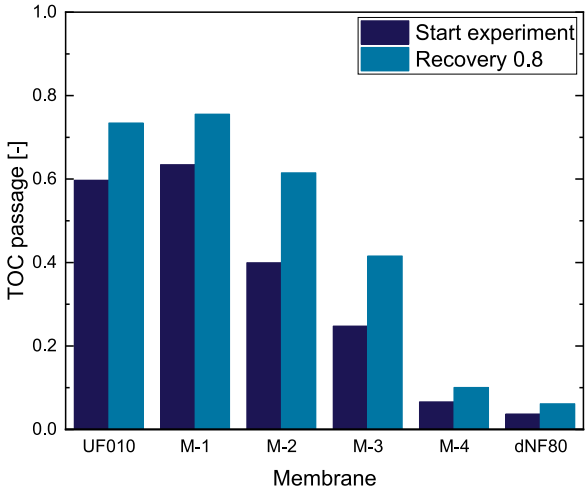

Fig. 6. Passage of TOC for the used membranes at the start of the experiment and at a recovery of 0.8.

In the LC-OCD analysis, the TOC is separated into different fractions, as can be seen in Table S5. The analysis shows that the humic substances are the largest fraction of the feed, ranging between 62% and 67%. The passage of humic substances follows the same pattern as the TOC. The humic substances are not detectable anymore in the permeate of the dNF80 membrane, independent of the recovery in this study. The only TOC still found in the permeate of the dNF80 are smaller organic molecules with a molecular weight below 500 g mol^{-1}. However, they still only have a passage of 20%. These results are in line with the expectations based on the MWCO results, and comparable to values for NF membranes reported in literature [66].

4.5. *Specific energy consumption analysis*

The obtained results from the experiments are translated into a prediction of the specific energy consumption (SEC) of the full process to be able to remove 70 or 80% of the OMPs with the oxidation step. The

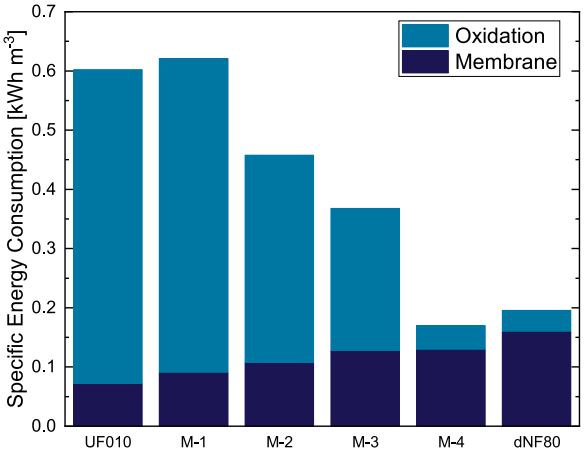

Fig. 7. Specific energy consumption for different membranes at a recovery of 80%, combined with oxidation with target OMP removal of 70%.

results of the calculated SEC are reported in Fig. 7, for a membrane recovery of 0.8 and a crossflow velocity of 0.3 ms^{-1}, and a targeted OMP removal of 70% with the oxidation step. The main differences in energy consumption are determined by the transmittance of the permeate for the oxidation, and the power of the recirculation pump in the NF step. The latter is caused by the fact that all membranes are assumed to operate around 2 bar and therefore use approximately the same amount of energy for permeation. However, the single-pass recovery is lower for denser membranes and therefore will lead to a higher flow through the recirculation pump and a correspondingly higher energy consumption.

It is clear that the more dense membranes tested in this work are able to decrease the energy consumption of the UV/H_2O_2 process significantly compared to more open membranes. The increase in required membrane energy for denser membranes is lower than the decrease of the SEC of the oxidation step. The M-4 membrane presents the best balance between permeability and transmittance improvement. Under these conditions, the energy consumption of the combined process can go down to 0.17 $kWhm^{-3}$ for 70% removal, and 0.18 $kWhm^{-3}$ for 80% removal. This value is also clearly lower compared to applying oxidation on effluent with a transmittance of around 50% (0.57–0.64 $kWhm^{-3}$ for 70 or 80% removal, respectively). Also, compared to using only a denser nanofiltration membrane, such as a dNF40 membrane by NX Filtration, the value for the combination is lower. With the same method for the calculations, 0.24 $kWhm^{-3}$ is obtained for a membrane that is able to retain 80% of a selection of OMPs [67]. However, in this case, the OMPs will end up in the concentrate and need to be treated further for actual removal.

The specific energy consumption in this section is a prediction and can vary for different conditions. For example, the recovery can influence the quality of the permeate as shown before, and with that, also the energy needed to drive the UV/H_2O_2 process. For the denser membranes, this does not lead to significant changes in the combined energy consumption. For 50% recovery, the values for the M-4 membrane slightly increase to 0.19–0.20 $kWhm^{-3}$ for 70% or 80% removal, respectively. For 90% recovery, the energy consumption equals 0.20–0.21 $kWhm^{-3}$ for 70 and 80% removal, respectively. An increase in recovery leads to a higher energy requirement for the oxidation step, due to lower permeate quality. However, this is in the calculations balanced by a smaller feed volume for the membrane system at higher recovery. This is because the calculations assume a permeate flow independent of recovery, as shown in Equation (9). It is taken into account that the concentrate of the membranes is returned to the preceding treatment step, and thus in the end comes back as feed for the membranes, as also shown in Figure S3. On the other hand, a lower recovery leads to a higher SEC for the membrane part due to a larger feed flow, but this is not balanced by the decrease in SEC of the oxidation step because of higher transmittance.

The energy consumption of the oxidation step depends, as shown before, mainly on transmittance, as well as on the targeted removal efficiency. The transmittance is important for the choice of membranes, as shown above. However, the targeted removal efficiency of 70 or 80% hardly matters at the more dense membranes, since the hydraulic maximum of the reactor is (almost) reached. At the more open membranes, it can be derived from Fig. 1 that this leads to a difference of 15% in the energy consumption in the oxidation step at maximum, which is in the same order of magnitude as the calculations in general. Since the combinations with the lowest energy consumption have the largest contribution from the membrane part, the remaining sensitivity analysis will focus on that part.

The effect of the crossflow velocity on the energy consumption of the combined system with an M-4 membrane is shown in Fig. 8. For simplicity, it is assumed that the crossflow velocity has no influence on the permeate quality, and therefore on the energy requirements of the oxidation. It is clear from Fig. 8 that the crossflow velocity has a major impact on the energy consumption of the process, since an increase from 0.2 to 0.5 ms^{-1} leads to a doubling of the SEC, from 0.14 to 0.28

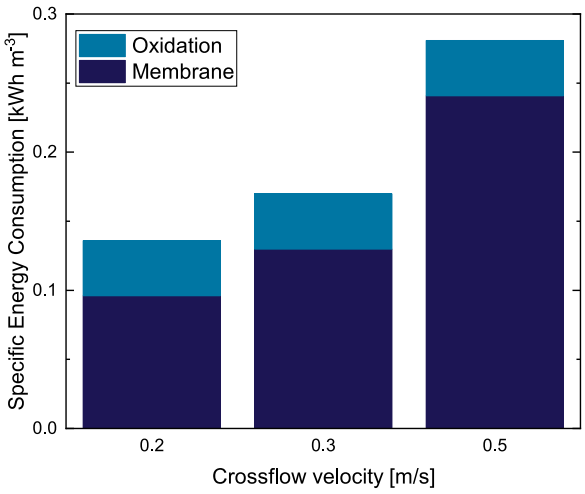

Fig. 8. Specific energy consumption for the M-4 membrane at a recovery of 80% with different crossflow velocities, combined with oxidation with target OMP removal of 70%.

$kWhm^{-3}$. This makes sense as most of the energy for this more dense membrane comes from the recirculation pump, as the single pass recovery is low in the feed & bleed mode. It is thus important to identify the lowest crossflow velocity that still leads to stable operation. Furthermore, the results show that the energy consumption of the combined system can potentially go lower than the previously mentioned 0.17 $kWhm^{-3}$, which was based on a crossflow velocity of 0.3 ms^{-1}. Apart from the crossflow velocity, a smart strategy for staging instead of using all membranes parallel could lead to lower energy consumption. Furthermore, the chosen permeability and flux also influence energy consumption. They are based on the best knowledge currently available, the experiments with effluent. However, the permeability can highly depend on the degree of foulants in the water and on the temperature.

The energy consumption of a process to remove OMPs is for a potential end-user only part of the bill; for a full scope, the entire operational and capital expenditures should be taken into account and preferably also environmental aspects, such as the CO_2-footprint. Since these parameters can highly vary from case to case, it is chosen to report SEC here. However, for the membrane part it can be commented that the denser the membrane gets, the lower the chosen flux is in the calculations and therefore, the more membrane area is required. A full-scale process for a denser membrane will thus consist of more membrane modules with a higher capital expenditure. On the other hand, permeate with a higher transmittance leads to less demanding conditions for the oxidation step, reducing CAPEX and OPEX. With an increasing reactor capacity for an increasing transmittance, as discussed in the methodology, fewer reactors are needed for a given flow. The costs for lamp replacement and total energy consumption are directly related to the number of reactors. The hydrogen peroxide consumption is directly related to the flow itself, but is affected by transmittance and composition.

The energy consumption presented for the oxidation in this article is significantly lower than reported by several other research articles for an equal UVC dose or similar performance on overlapping OMPs. At a transmittance of more than 80%, the energy consumption predicted was approximately 50–80% less than in two other cases [68,69]. This could be explained by the design of the reactor and choice of UVC lamps, which utilize the energy input better [31]. The value for only oxidation with UV/H_2O_2 is similar to other findings [70], with 0.7–2.28 $kWhm^{-3}$ on wastewater effluent, depending on used path length. The estimation for only NF of 0.24 $kWhm^{-3}$ is comparable to other findings for hollow fiber NF on surface water [71,72].

Besides the comparison to the same technologies in literature, a comparison can also be made to other technologies. A wide range of estimates can be found in literature, e.g. in [7,15,73,74]. Mousel et al. collected data from several full-scale WWTPs and found an average SEC of 0.08 $kWhm^{-3}$ for adsorption and 0.08–0.11 $kWhm^{-3}$ for ozonation, if only the electrical energy demand at the WWTP itself was considered [74]. These values are lower than what is reported here. Important parameters that are not taken into account in these values, but take a considerable amount of energy, are the production of oxygen for ozonation, and the production of active carbon from raw coal. This makes the cumulative energy demand for adsorption up to 1.78 $kWhm^{-3}$ or 0.16 $kWhm^{-3}$ for ozonation. The scope of this work is limited to direct energy consumption. For instance, the energy consumption required for the production of hydrogen peroxide is not included. However, it is clear that the range reported in this work is competitive with other processes. This, together with the fact that two different processes are combined and thus two different barriers for pollutants leading to a potentially very clean product water, creates a promising process for further research.

5. Conclusion

This work provides insight into the synergistic energy savings of a combination of NF with UV/H_2O_2 oxidation to remove OMPs from the effluent of a wastewater treatment plant. The hypothesis was that a combined technology could potentially exceed the performance of one single technology when both technologies are well adapted to each other while offering a double barrier. To get to this end, several hollow fiber membranes were characterized, ranging from ultrafiltration membranes with a reported MWCO of around 10 kDa to NF membranes with a reported MWCO of around 800 Da. In this research, it was shown that the MWCO is actually not a single value for a membrane, but depends on the conditions during measuring. In the case of this work, it depended strongly on the applied flux. For more open membranes, the MWCO increases with flux, while it decreases for more dense membranes with increasing flux, which is mainly attributed to concentration polarization playing a larger role for larger molecules. Furthermore, the membranes were tested with WWTP effluent to get insight into the increase in transmittance that can be obtained, showing that a major increase in transmittance was obtained between membranes M-3 and M-4. This increase in transmittance can be explained by the substantially lower passage of humic acids through the M-4 membrane, as evidenced by the LC-OCD measurements.

Taking the experimental data of the membranes and existing data from oxidation processes, the energy analysis shows that a slightly more open NF membrane is able to create the lowest energy consumption of the full system with a base case of 0.17 $kWhm^{-3}$ with potential to go as low as 0.13 $kWhm^{-3}$, whilst producing clean water with high transmittance and removing 70% of a selection of micropollutants, while an increase to 80% removal only requires 0.01 $kWhm^{-3}$ additional energy. This is clearly lower compared to using oxidation to treat raw effluent, and also slightly lower compared to an estimation for only using a denser NF membrane to remove OMPs. This value is comparable to other values for energy consumption of OMP-removing technologies found in literature. Overall, the combined process of NF and UV/H_2O_2 oxidation has the potential to create high-quality water with possibilities for reuse with competitive energy consumption and offering two barriers at the same time. This work can act as a stepping stone towards more detailed future investigations, including experimental demonstration of the full concept.

CRediT authorship contribution statement

Hans David Wendt: Writing – original draft, Visualization, Validation, Investigation. **I. Sena Yaltur:** Writing – review & editing, Investigation. **Dennis M. Reurink:** Writing – review & editing, Supervision. **Clara Thege:** Writing – review & editing, Writing – original draft, Methodology. **Kaspar Groot Kormelinck:** Writing – review & editing, Methodology, Conceptualization. **Joris de Grooth:** Writing – review & editing, Supervision, Conceptualization.

Declaration of Competing Interest

The authors declare that they have no known competing financial interests or personal relationships that could have appeared to influence the work reported in this paper.

Data availability

Data will be made available via 4TU.data after acceptance/publication.

Acknowledgments

Hans David Wendt acknowledges funding received from NWO domain Applied and Engineering Sciences (TTW), grant number 17744. This funding was partly made possible through small cash and/or in-kind contributions of KWR Watercycle Research Institute, NX Filtration, Nijhuis Water Technology, Oasen, Saxion, Waterkracht, Waterboard Aa en Maas, Waterboard Vallei en Veluwe and STOWA. Sena Yaltur, Dennis Reurink, Joris de Grooth, Clara Thege and Kaspar Groot Kormelinck acknowledge funding received from the ERDF (European Regional Development Fund), project NanoX (PROJ-01023), which has partly financed their contributions.

Appendix A. Supporting information

Supplementary data associated with this article can be found in the online version at doi:10.1016/j.jece.2024.112997.

References

[1] I. Michael, L. Rizzo, C.S. McArdell, C.M. Manaia, C. Merlin, T. Schwartz, C. Dagot, D. Fatta-Kassinos, Urban wastewater treatment plants as hotspots for the release of antibiotics in the environment: a review, Water Res. 47 (3) (2013) 957–995, https://doi.org/10.1016/j.watres.2012.11.027.
[2] R.I.L. Eggen, J. Hollender, A. Joss, M. Schärer, C. Stamm, Reducing the discharge of micropollutants in the aquatic environment: the benefits of upgrading wastewater treatment plants, Environ. Sci. Technol. 48 (14) (2014) 7683–7689, https://doi.org/10.1021/es500907n.
[3] Y. Luo, W. Guo, H.H. Ngo, L.D. Nghiem, F.I. Hai, J. Zhang, S. Liang, X.C. Wang, A review on the occurrence of micropollutants in the aquatic environment and their fate and removal during wastewater treatment, Sci. Total Environ. 473-474 (2014) 619–641, https://doi.org/10.1016/j.scitotenv.2013.12.065.
[4] K. Peschke, J. Geburzi, H.R. Korhler, K. Wurm, R. Triebskorn, Invertebrates as indicators for chemical stress in sewage-influenced stream systems: toxic and endocrine effects in gammarids and reactions at the community level in two tributaries of Lake Constance, Schussen Argen. Ecotoxicol. Environ. Saf. 106 (2014) 115–125, https://doi.org/10.1016/j.ecoenv.2014.04.011.
[5] L. Wolska, M. Cieszynska-semenowicz, W. Ratajczyk, Micropollutants in treated wastewater, Ambio 49 (2) (2020) 487–503, https://doi.org/10.1007/s13280-019-01219-5.
[6] Y. Yang, Y.S. Ok, K.H. Kim, E.E. Kwon, Y.F. Tsang, Occurrences and removal of pharmaceuticals and personal care products (PPCPs) in drinking water and water/sewage treatment plants: a review, Sci. Total Environ. 596-597 (2017) 303–320, https://doi.org/10.1016/j.scitotenv.2017.04.102.
[7] K. Kosek, A. Luczkiewicz, S. Fudala-Książek, K. Jankowska, M. Szopińska, O. Svahn, J. Tränckner, A. Kaiser, V. Langas, E. Björklund, Implementation of advanced micropollutants removal technologies in wastewater treatment plants (WWTPs) - Examples and challenges based on selected EU countries, Environ. Sci. Policy 112 (April) (2020) 213–226, https://doi.org/10.1016/j.envsci.2020.06.011.
[8] S. de Boer, J. González-Rodríguez, J.J. Conde, M.T. Moreira, Benchmarking tertiary water treatments for the removal of micropollutants and pathogens based on operational and sustainability criteria, J. Water Process Eng. 46 (2021) (2022), https://doi.org/10.1016/j.jwpe.2022.102587.
[9] T. Krahnstöver, N. Santos, K. Georges, L. Campos, B. Antizar-Ladislao, Low-carbon technologies to remove organic micropollutants from wastewater: a focus on pharmaceuticals, Sustainability 14 (18) (2022), https://doi.org/10.3390/su141811686.
[10] K. Arola, B. Van der Bruggen, M. Mänttäri, M. Kallioinen, Treatment options for nanofiltration and reverse osmosis concentrates from municipal wastewater

treatment: a review, Crit. Rev. Environ. Sci. Technol. 49 (22) (2019) 2049–2116, https://doi.org/10.1080/10643389.2019.1594519.
[11] F.E. Titchou, H. Zazou, H. Afanga, J. ElGaayda, R. AitAkbour, P.V. Nidheesh, M. Hamdani, Removal of organic pollutants from wastewater by advanced oxidation processes and its combination with membrane processes, Chem. Eng. Process. - Process. Intensif. 169 (September) (2021) 108631, https://doi.org/10.1016/j.cep.2021.108631.
[12] A. Azaïs, J. Mendret, E. Petit, S. Brosillon, Influence of volumetric reduction factor during ozonation of nanofiltration concentrates for wastewater reuse, Chemosphere 165 (2016) 497–506, https://doi.org/10.1016/j.chemosphere.2016.09.071.
[13] J.L. Acero, F.J. Benitez, F.J. Real, F. Teva, Micropollutants removal from retentates generated in ultrafiltration and nanofiltration treatments of municipal secondary effluents by means of coagulation, oxidation, and adsorption processes, Chem. Eng. J. 289 (2016) 48–58, https://doi.org/10.1016/j.cej.2015.12.082.
[14] P. Liu, H. Zhang, Y. Feng, F. Yang, J. Zhang, Removal of trace antibiotics from wastewater: a systematic study of nanofiltration combined with ozone-based advanced oxidation processes, Chem. Eng. J. 240 (2014) 211–220, https://doi.org/10.1016/j.cej.2013.11.057.
[15] L. Rizzo, S. Malato, D. Antakyali, V.G. Beretsou, M.B. Dolić, W. Gernjak, E. Heath, I. Ivancev-Tumbas, P. Karaolia, A.R. LadoRibeiro, G. Mascolo, C.S. McArdell, H. Schaar, A.M.T. Silva, D. Fatta-Kassinos, Consolidated vs new advanced treatment methods for the removal of contaminants of emerging concern from urban wastewater, Sci. Total Environ. 655 (August 2018) (2019) 986–1008, https://doi.org/10.1016/j.scitotenv.2018.11.265.
[16] M. Saquib, C. Vinckier, B. van der Bruggen, The effect of UF on the efficiency of O_3/H_2O_2 for the removal of organics from surface water, Desalination 260 (1–3) (2010) 39–42, https://doi.org/10.1016/j.desal.2010.05.003.
[17] E.M. Cuerda-Correa, M.F. Alexandre-Franco, C. Fernández-González, Advanced oxidation processes for the removal of antibiotics from water. An overview, Water 12 (1) (2020) 102, https://doi.org/10.3390/w12010102.
[18] D.B. Miklos, C. Remy, M. Jekel, K.G. Linden, J.E. Drewes, U. Hübner, Evaluation of advanced oxidation processes for water and wastewater treatment - A critical review, Water Res. 139 (2018) 118–131, https://doi.org/10.1016/j.watres.2018.03.042.
[19] S. Szerzyna, M. Mołczan, M. Wolska, W. Adamski, and J. Wiśniewski.Absorbance based water quality indicators as parameters for treatment process control with respect to organic substance removal.In: E3S Web Conf., volume 17, 2017.10.1051/e3sconf/20171700091.
[20] B.P. Chaplin, Critical review of electrochemical advanced oxidation processes for water treatment applications, Environ. Sci. Process. Impacts 16 (6) (2014) 1182–1203, https://doi.org/10.1039/c3em00679d.
[21] W.A. Jonkers, E.R. Cornelissen, W.M. de Vos, Hollow fiber nanofiltration: from lab-scale research to full-scale applications, J. Memb. Sci. 669 (November 2022) (2023) 121234, https://doi.org/10.1016/j.memsci.2022.121234.
[22] S. Sethi, M.R. Wiesner, Simulated cost comparisons of hollow-fiber and integrated nanofiltration configurations, Water Res. 34 (9) (2000) 2589–2597, https://doi.org/10.1016/S0043-1354(00)00017-8.
[23] C. Kappel, A.J.B. Kemperman, H. Temmink, A. Zwijnenburg, H.H.M. Rijnaarts, K. Nijmeijer, Impacts of NF concentrate recirculation on membrane performance in an integrated MBR and NF membrane process for wastewater treatment, J. Memb. Sci. 453 (2014) 359–368, https://doi.org/10.1016/j.memsci.2013.11.023.
[24] F. Soltermann, C. Abegglen, C. Götz, U. VonGunten, Bromide sources and loads in Swiss surface waters and their relevance for bromate formation during wastewater ozonation, Environ. Sci. Technol. 50 (18) (2016) 9825–9834, https://doi.org/10.1021/acs.est.6b01142.
[25] S. Yoon, H. Tanaka, Formation of N-nitrosamines by chloramination or ozonation of amines listed in pollutant release and transfer registers (PRTRs), Chemosphere 95 (2014) 88–95, https://doi.org/10.1016/j.chemosphere.2013.07.090.
[26] M. Sgroi, F.G.A. Vagliasindi, S.A. Snyder, P. Roccaro, N-Nitrosodimethylamine (NDMA) and its precursors in water and wastewater: a review on formation and removal, Chemosphere 191 (2018) 685–703, https://doi.org/10.1016/j.chemosphere.2017.10.089.
[27] W.L. Wang, Q.Y. Wu, N. Huang, Z.B. Xu, M.Y. Lee, H.Y. Hu, Potential risks from UV/H_2O_2 oxidation and UV photocatalysis: a review of toxic, assimilable, and sensory-unpleasant transformation products, Water Res. 141 (2018) 109–125, https://doi.org/10.1016/j.watres.2018.05.005.
[28] A. Cibati, R. Gonzalez-Olmos, S. Rodriguez-Mozaz, G. Buttiglieri, Unravelling the performance of UV/H_2O_2 on the removal of pharmaceuticals in real industrial, hospital, grey and urban wastewaters, Chemosphere 290 (October 2021) (2022) 133315, https://doi.org/10.1016/j.chemosphere.2021.133315.
[29] C. Baresel, M. Harding, and C. Junestedt.Removal of pharmaceutical residues from municipal wastewater using UV/H2O2. Technical Report September, 2019.⟨https://urn.kb.se/resolve?urn=urn:nbn:se:ivl:diva-2828⟩.
[30] A.M. Parker, Y. Lester, E.K. Spangler, U. von Gunten, K.G. Linden, UV/H_2O_2 advanced oxidation for abatement of organophosphorous pesticides and the effects on various toxicity screening assays, Chemosphere 182 (2017) 477–482, https://doi.org/10.1016/j.chemosphere.2017.04.150.
[31] R. Hofman-Caris, D. Harmsen, and B. Wols.Additional UV/H_2O_2 treatment for removal of polar organic micropollutants at Drinking water production site Heel. KWR Report 2015.082. Technical Report October, 2015.⟨https://edepot.wur.nl/459288⟩.
[32] Direct Nanofiltration Membranes.2024 ⟨https://nxfiltration.com/products/nano/⟩.
[33] J. de Grooth, R. Oborný, J. Potreck, K. Nijmeijer, W.M. de Vos, The role of ionic strength and odd-even effects on the properties of polyelectrolyte multilayer nanofiltration membranes, J. Memb. Sci. 475 (2015) 311–319, https://doi.org/10.1016/j.memsci.2014.10.044.
[34] S. Platt, M. Mauramo, S. Butylina, M. Nyström, Retention of pegs in cross-flow ultrafiltration through membranes, Desalination 149 (1-3) (2002) 417–422, https://doi.org/10.1016/S0011-9164(02)00767-1.
[35] R.W. Baker, Membrane Technology an Applications, John Wiley & Sons, Ltd, 2004.
[36] S.A. Huber, F.H. Frimmel, Flow injection analysis of organic and inorganic carbon in the low-ppb range, Anal. Chem. 63 (19) (1991) 2122–2130, https://doi.org/10.1021/ac00019a011.
[37] S.A. Huber, A. Balz, M. Abert, W. Pronk, Characterisation of aquatic humic and non-humic matter with size-exclusion chromatography - organic carbon detection - organic nitrogen detection (LC-OCD-OND), Water Res. 45 (2) (2011) 879–885, https://doi.org/10.1016/j.watres.2010.09.023.
[38] G. Towler and R. Sinnott.Transport and Storage of Fluids.2013.10.1016/b978-0-08-096659-5.00020-1.
[39] D. Li, Z. Feng, B. Zhou, H. Chen, R. Yuan, Impact of water matrices on oxidation effects and mechanisms of pharmaceuticals by ultraviolet-based advanced oxidation technologies: a review, Sci. Total Environ. 844 (July) (2022) 157162, https://doi.org/10.1016/j.scitotenv.2022.157162.
[40] B.A. Wols, D.J.H. Harmsen, E.F. Beerendonk, C.H.M. Hofman-Caris, Predicting pharmaceutical degradation by UV (LP)/H_2O_2 processes: a kinetic model, Chem. Eng. J. 255 (2014) 334–343, https://doi.org/10.1016/j.cej.2014.05.088.
[41] W. Kowalski, Ultraviolet Germicidal Irradiation Handbook, Springer, 2009, https://doi.org/10.1007/978-3-642-01999-9.
[42] B.A. Wols, J.A.M.H. Hofman, E.F. Beerndonk, W.S.J. Uijttewaal, J.C. van Dijk, A systematic approach for the design of UV reactors using computational fluid dynamics, arXiv:arXiv:0201037v1, AIChE J. 57 (1) (2011) 193–207, https://doi.org/10.1002/aic.12255.
[43] Metcalf, Eddy. Wastewater Engineering: Treatment and Resource Recovery, 5th edition, McGraw-Hill, New York, 2014 (editors.).
[44] J.L. Weishaar, G.R. Aiken, B.A. Bergamaschi, M.S. Fram, R. Fujii, K. Mopper, Evaluation of specific ultraviolet absorbance as an indicator of the chemical composition and reactivity of dissolved organic carbon, Environ. Sci. Technol. 37 (20) (2003) 4702–4708, https://doi.org/10.1021/es030360x.
[45] T.A. Doane, W.R. Horwáth, Eliminating interference from iron(III) for ultraviolet absorbance measurements of dissolved organic matter, Chemosphere 78 (11) (2010) 1409–1415, https://doi.org/10.1016/j.chemosphere.2009.12.062.
[46] B.A. Wols, C.H.M. Hofman-Caris, Review of photochemical reaction constants of organic micropollutants required for UV advanced oxidation processes in water, Water Res. 46 (9) (2012) 2815–2827, https://doi.org/10.1016/j.watres.2012.03.036.
[47] M. Saleem, N.G. Choi, K.H. Lee, Facile synthesis of an optical sensor for CO_3^{2-} and HCO_3^- detection, Int. J. Environ. Anal. Chem. 95 (7) (2015) 592–608, https://doi.org/10.1080/03067319.2015.1046056.
[48] J. Mack, J.R. Bolton, Photochemistry of nitrite and nitrate in aqueous solution: A review, J. Photochem. Photobiol. A Chem. 128 (1-3) (1999) 1–13, https://doi.org/10.1016/S1010-6030(99)00155-0.
[49] H. Galal-Gorchev, J.C. Morris, Formation and Stability of Bromamide, Bromimide, and Nitrogen Tribromide in Aqueous Solution, Inorg. Chem. 4 (6) (1965) 899–905, https://doi.org/10.1021/ic50028a029.
[50] Y. Peng, S. Fu, H. Liu, L.A. Lucia, Determining esterase activity via the isosbestic point of p-nitrophenol, BioResources 11 (4) (2016) 10099–10111, https://doi.org/10.15376/biores.11.4.10099-10111.
[51] A.L. Riscassi, T.M. Scanlon, Controls on stream water dissolved mercury in three mid-Appalachian forested headwater catchments, Water Resour. Res. 47 (12) (2011) 1–16, https://doi.org/10.1029/2011WR010977.
[52] F.P. Chaves, G. Gomes, A. Della-Flora, A. Dallegrave, C. Sirtori, E.M. Saggioro, D. M. Bila, Comparative endocrine disrupting compound removal from real wastewater by UV/Cl and UV/H2O2: Effect of pH, estrogenic activity, transformation products and toxicity, Sci. Total Environ. 746 (2020) 141041, https://doi.org/10.1016/j.scitotenv.2020.141041.
[53] Y. Huo, M. Li, Z. An, J. Jiang, Y. Zhou, Y. Ma, J. Xie, F. Wei, M. He, Effect of pH on UV/H_2O_2-mediated removal of single, mixed and halogenated parabens from water, J. Hazard. Mater. 462 (October 2023) (2024) 132818, https://doi.org/10.1016/j.jhazmat.2023.132818.
[54] S.L. Ulliman, G. McKay, F.L. Rosario-Ortiz, K.G. Linden, Low levels of iron enhance UV/H_2O_2 efficiency at neutral pH, Water Res. 130 (2018) 234–242, https://doi.org/10.1016/j.watres.2017.11.041.
[55] N.T. Hoang, F.M. Mwazighe, The various effects of hydrogen phosphate and bicarbonate in the degradation of some pollutants in the UV/chlorine and the UV/H_2O_2 processes, J. Water Process Eng. 57 (June 2023) (2024) 104646, https://doi.org/10.1016/j.jwpe.2023.104646.
[56] Proposal for a revised Urban Wastewater Treatment Directive - Directorate-General for Environment of European Comission, 2022.⟨https://environment.ec.europa.eu/publications/proposal-revised-urban-wastewater-treatment-directive_en⟩.
[57] B.J. van Weeren.The Innovation Program Removal of Micropollutants at Wastewater Treatment Plants: the State of Affairs Autumn 2021. Technical report, STOWA, 2021.⟨https://www.stowa.nl/onderwerpen/waterkwaliteit/nieuwe-stoffen/innovation-program-removal-micropollutants-wastewater⟩.
[58] G. Dagher, G. Saab, A. Martin, G. Couturier, P. Candido, L. Moulin, J.P. Crou, Understanding and predicting the adsorption and rejection of pesticides and metabolites by hollow fiber nanofiltration membranes, Sep. Purif. Technol. 330 (125323) (2024), https://doi.org/10.1016/j.seppur.2023.125323.
[59] M.T. Sturm, E. Myers, D. Schober, C. Thege, A. Korzin, K. Schuhen, Adaptable process design as a key for sustainability upgrades in wastewater treatment: comparative study on the removal of micropollutants by advanced oxidation and

granular activated carbon processing at a German municipal wastewater treatment plant, Sustainability 14 (18) (2022), https://doi.org/10.3390/su141811605.
[60] B.A. Wols, D.J.H. Harmsen, T. van Remmen, E.F. Beerendonk, C.H.M. Hofman-Caris, Design aspects of UV/H_2O_2 reactors, Chem. Eng. Sci. 137 (2015) 712–721, https://doi.org/10.1016/j.ces.2015.06.061.
[61] B.A. Wols, D.J.H. Harmsen, J. Wanders-Dijk, E.F. Beerendonk, C.H.M. Hofman-Caris, Degradation of pharmaceuticals in UV (LP)/H_2O_2 reactors simulated by means of kinetic modeling and computational fluid dynamics (CFD), Water Res. 75 (0) (2015) 11–24, https://doi.org/10.1016/j.watres.2015.02.014.
[62] J. Shirley, S. Mandale, V. Kochkodan, Influence of solute concentration and dipole moment on the retention of uncharged molecules with nanofiltration, Desalination 344 (2014) 116–122, https://doi.org/10.1016/j.desal.2014.03.024.
[63] H.J. Zwijnenberg, S.M. Dutczak, M.E. Boerrigter, M.A. Hempenius, M.W.J. Luiten-Olieman, N.E. Benes, M. Wessling, D. Stamatialis, Important Factors Influ. Mol. Weight Cut. - Determ. Membr. Org. Solvents 390-391 (2012) 211–217, https://doi.org/10.1016/j.memsci.2011.11.039.
[64] R.W. Baker, Methods of fractionating polymers by ultrafiltration, J. Appl. Polym. Sci. 13 (2) (1969) 369–376, https://doi.org/10.1002/app.1969.070130210.
[65] M.A. Junker, W.M. de Vos, J. de Grooth, R.G.H. Lammertink, Relating uncharged solute retention of polyelectrolyte multilayer nanofiltration membranes to effective structural properties, J. Memb. Sci. 668 (November 2022) (2023) 121164, https://doi.org/10.1016/j.memsci.2022.121164.
[66] S. Meylan, F. Hammes, J. Traber, E. Salhi, U. von Gunten, W. Pronk, Permeability of low molecular weight organics through nanofiltration membranes, Water Res. 41 (17) (2007) 3968–3976, https://doi.org/10.1016/j.watres.2007.05.031.
[67] S.B. Rutten, V.L. Levering, L. HernándezLeal, J. de Grooth, H.D.W. Roesink, Retention of micropollutants by polyelectrolyte multilayer based hollow fiber nanofiltration membranes under fouled conditions, J. Water Process Eng. 53 (March) (2023) 103760, https://doi.org/10.1016/j.jwpe.2023.103760.
[68] J.C. Kruithof, B.J. Martijn, UV/H2O2 treatment: an essential process in a multi barrier approach against trace chemical contaminants, 2, Water Supply 13 (1) (2013) 130–138, https://doi.org/10.2166/ws.2012.091, 2.
[69] I.H. Kim, N. Yamashita, Y. Kato, H. Tanaka, Discussion on the application of UV/H_2O_2, O_3 and O_3/UV processes as technologies for sewage reuse considering the removal of pharmaceuticals and personal care products, 3, Water Sci. Technol. 59 (5) (2009) 945–955, https://doi.org/10.2166/wst.2009.076, 3.
[70] I.A. Katsoyiannis, S. Canonica, U. von Gunten, Efficiency and energy requirements for the transformation of organic micropollutants by ozone, O_3/H_2O_2 and UV/H_2O_2, Water Res. 45 (13) (2011) 3811–3822, https://doi.org/10.1016/j.watres.2011.04.038.
[71] A. Keucken, Y. Wang, K.H. Tng, G. Leslie, T. Spanjer, S.J. Köhler, Optimizing hollow fibre nanofiltration for organic matter rich lake water, Water 8 (10) (2016), https://doi.org/10.3390/w8100430.
[72] J. Jährig, L. Vredenbregt, D. Wicke, U. Miehe, A. Sperlich, Capillary nanofiltration under anoxic conditions as post-treatment after bank filtration, Water 10 (11) (2018), https://doi.org/10.3390/w10111599.
[73] D. Li, Z. Feng, B. Zhou, H. Chen, R. Yuan, Impact of water matrices on oxidation effects and mechanisms of pharmaceuticals by ultraviolet-based advanced oxidation technologies: A review, Sci. Total Environ. 844 (June) (2022) 157162, https://doi.org/10.1016/j.scitotenv.2022.157162.
[74] D. Mousel, L. Palmowski, J. Pinnekamp, Energy demand for elimination of organic micropollutants in municipal wastewater treatment plants, Sci. Total Environ. 575 (2017) 1139–1149, https://doi.org/10.1016/j.scitotenv.2016.09.197.